JOURNAL OF NATURAL PRODUCTS

Article

Cite This: J. Nat. Prod. XXXX, XXX, XXX−XXX

pubs.acs.org/jnp

Phytochemical Study of *Senecio volckmannii* Assisted by CASE-3D with Residual Dipolar Couplings and Isotropic $^{1}H/^{13}C$ NMR Chemical Shifts

Sebastián J. Castro,[†] Manuela E. García,[*,†] José M. Padrón,[‡] Armando Navarro-Vázquez,[∥] Roberto R. Gil,[§] and Viviana E. Nicotra[*,†]

[†]Facultad de Ciencias Químicas, Instituto Multidisciplinario de Biología Vegetal (IMBIV-CONICET), Universidad Nacional de Córdoba, Casilla de Correo 495, 5000 Córdoba, Argentina

[‡]BioLab, Instituto Universitario de Bio-Orgánica "Antonio González" (IUBO-AG), Centro de Investigaciones Biomédicas de Canarias (CIBICAN), Universidad de La Laguna, C/Astrofísico Francisco Sánchez 2, 38206 La Laguna, Spain

[§]Department of Chemistry, Carnegie Mellon University, 4400 Fifth Avenue, Pittsburgh, Pennsylvania 15213, United States

[∥]Departamento de Química Fundamental, CCEN, Universidade Federal de Pernambuco, Avenida Professor Moraes Rego, 1235, Cidade Universitáaria, 50670-901 Recife, PE, Brazil

Supporting Information

ABSTRACT: Nine new eremophilanolides, with seven known sesquiterpenoids, and 4-hydroxyacetophenone were isolated from the aerial parts of *Senecio volckmannii* var. *volckmannii*. The structures of these compounds were fully characterized using a combination of spectroscopic techniques including multinuclear and multidimensional NMR and mass spectrometry. The recently published Computer Assisted 3D Structure Elucidation (CASE-3D) protocol was applied in the configurational and conformational analysis of many of these eremophilanolides on the basis of Residual Dipolar Couplings (RDCs) and/or DFT predicted $^{1}H/^{13}C$ chemical shifts.

Senecio (Asteraceae) is a genus that is found worldwide except in the Pacific islands and the Antarctic continent. The highest concentration of species is in the mountain regions of America, Africa, and Asia. Recently, 262 *Senecio* species have been recorded in Argentina, most of them in the Altoandina phytogeographical province.[1]

The chemical composition of the *Senecio* genus has been widely investigated. Pyrrolizidine alkaloids and eremophilane-type sesquiterpenoids are among the most frequently found secondary metabolites in this genus. Pyrrolizidine alkaloids are well-known for their poisonous effects to cattle and humans.[2,3] Sesquiterpenoids with an eremophilane-type skeleton have shown cytotoxic, antibacterial, antifungal, anti-inflammatory, trypanocidal, and plant growth regulatory activities, among others.[4,5]

Senecio volckmannii Phil. (syn. *S. rosmarinus* Phil.var. *rosmarinus, S. rosmarinus* Phil. var. *ascotanensis, S. spegazzinii* Cabrera) grows in the high mountains of Chile (Atacama, Coquimbo, Antofagasta) and Argentina (Jujuy to Neuquén).[6,7] It comprises two varieties: var. *pinohachensis* Tortosa & Bartoli, endemic to Argentina (Neuquén) and var. *volckmannii* with a wide distribution in Chile and Argentina. Previous chemical analyses of *S. volckmannii* (subnom. *S. rosmarinus*, now a synonym of *S. volckmannii* var. *volckmannii*) showed the presence of sesquiterpene lactones.[8] In the present study, we report the isolation of 17 compounds from *Senecio volckmannii* var. *volckmannii* (Figure 1), nine new eremophilane-type sesquiterpenoids (**1**−**9**) along with eight known constituents (**10**−**17**).

Received: February 21, 2018

DOI: 10.1021/acs.jnatprod.8b00162
J. Nat. Prod. XXXX, XXX, XXX−XXX

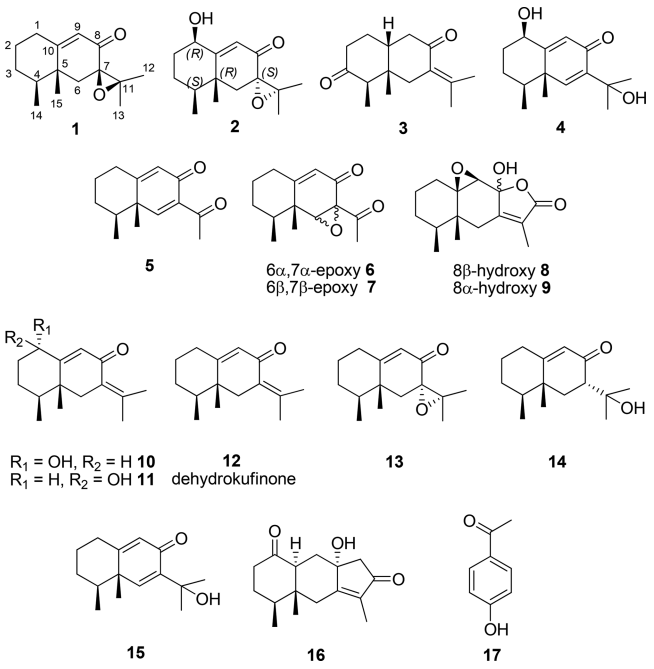

Figure 1. Compounds isolated from *Senecio volckmannii*.

RESULTS AND DISCUSSION

The CH_2Cl_2 extract of the aerial parts of *Senecio volckmannii* yielded nine new sesquiterpenoids: four sesquiterpenoids (**1**–**4**), three nor-sesquiterpenoids (**5**–**7**), two sesquiterpene lactones (**8** and **9**), and eight known compounds (**10**–**17**). The structures of the new compounds were elucidated on the basis of UV, IR, HRMS, and NMR data, while the structures of the known compounds were established by comparison of observed and reported NMR data.

The molecular formula of compound **1** was $C_{15}H_{23}O_2$ as assessed by HRESIMS data. The ^{1}H NMR spectrum of **1** showed a vinylic proton signal at δ 5.90 (d, J = 1.2 Hz) and four methyl signals at δ 1.31 s, 1.44 s, 1.13 s, and 0.99 (d, J = 6.6 Hz) (Table 1). The ^{13}C data displayed 15 signals corresponding to four methyl, four methylene, a carbonyl, an olefinic moiety, and two tertiary oxygenated carbons typical of an epoxy function (Table 2). The ^{1}H and ^{13}C NMR signals and the analysis of the COSY, HSQC, and HMBC spectra suggested the presence of an eremophilane skeleton closely related to ligudicin A (**13**),[9] indicating the same skeleton and substitution pattern (Figures S1-1–S1-5, Supporting Information). This is evident by the similarity in the ^{1}H and ^{13}C chemical shifts which are only slightly different in the vicinity of the C-4, C-5, and C-7 stereocenters. Indeed, the largest chemical shift differences between compounds **1** and **13** were observed at C-4, C-6, C-14, and C-15 which changed from δ 40.4, 37.3, 17.0, and 21.5 to δ 43.4, 40.4, 15.2, and 18.0, respectively. Most eremophilane sesquiterpenoids have been described as having β-oriented C-4 and C-5 methyl groups on the basis of biosynthetic considerations.[10,11]

The similarity in the NMR data of compounds **1** and **13** suggested that the structural difference could be restricted to the orientation of the 7,11-epoxy group. To confirm this assumption, a combination of NMR tools such as $^3J_{HH}$ coupling constants analysis, DQF-Phase Sensitive COSY, and Residual Dipolar Coupling (RDCs) were applied to compounds **1** and **13**. The ^{1}H NMR signal of H-4 in compound **13** was overlapped with the signals corresponding to H-3a, H-3b, and H-2b, preventing the direct extraction of J coupling constants from the 1D spectrum. However, this signal appeared without overlapping in compound **1**. Therefore, the coupling constants involving H-3a, H-3b, H-4, and CH_3-14 were extracted as follows: (a) A coupling constant of 6.6 Hz for H-4/CH_3-14 was directly extracted from the doublet at 0.99 ppm corresponding to CH_3-14; (b) A coupling constant of 4.1 Hz was directly extracted from the signal of H-4 and was assigned to a coupling of H-4 and one of the H-3 protons; (c) If the distance in Hz between the two outer peaks of the H-4 multiplet is 35.5 Hz and corresponds to the sum of all the coupling constants, then the other H-4/H-3 constant can be calculated as 35.5 − (6.6 × 3 + 4.1) = 11.6 Hz. This value is clearly indicating that H-4 is involved in a *trans*-diaxial relationship with one of the C-3 protons. These three J values together with the corresponding chemical shifts for H-3a, H-3b, H-4, and CH_3-14 were plugged into the spin simulation

Table 1. ^{1}H NMR Data of Compounds 1–9 in $CDCl_3$[a]

position	1	2	3	4	5	6	7	8	9
1a	2.46 dd (12.5,4.9)	4.35 brs	1.94 m	4.46 t (2.6)	2.44 m	2.35 m	2.26 m	1.95 m	1.94 m
1b	2.23brd (12.5)		1.69 m		2.38 m	2.22 m	2.12 m	1.01 m	1.12 m
2a	2.04 m	1.96 m	2.41 m	2.07 m	2.00 m	1.80 m	1.93 m	1.70 m	1.46 m
2b	1.43 m	1.68 m	2.41 m	1.62 m	1.41 m	1.38 m	1.38 m	1.21 m	Nd
3a	1.66 m	1.81 m		1.94 m	1.61 m	1.57 m	1.53 m	1.46 m	1.50 m
3b	1.50 m	1.36 m		1.47 m	1.61 m	1.39 m	1.35 m	1.21 m	1.15 m
4	1.76 m	1.48 m	1.90 m	1.51 m	1.55 m	1.87 m	1.69 m	1.22 m	1.73 m
6a	2.10 d (15.0)	2.07 d (13.7)	2.79 d (14.8)	6.86 s	7.67 s	3.42 brs	3.49 brs	2.43 d (13.0)	2.34 d (14.8)
6b	2.09 d (15.0)	1.94 d (13.7)	2.12 brd (14.8)					2.11 brd (13.0)	2.28 brd (14.8)
9a	5.90 d (1.2)	5.91 s	2.64 m	6.07 s	6.12 s	5.71 d (1.8)	5.74 brs	3.27 s	3.30 s
9b			2.40 m						
10			2.72 dd (12.6,4.2)						
12	1.31 s	1.24 s	2.01 d (2.2)	1.38[b]					
13	1.44 s	1.39 s	1.79 d (1.4)	1.39[b]	2.57 s	2.27 s	2.26 s	1.74 d (0.8)	1.73 d (1.6)
14	0.99 d (6.6)	0.89 d (6.8)	1.02 d (6.6)	1.04 d (6.7)	1.11 d (5.9)	1.05 d (6.8)	0.97 d (6.8)	0.87 d (6.0)	0.92 d (6.8)
15	1.13 s	1.28 s	0.71 s	1.26 s	1.19 s	1.15 s	1.24 s	1.07 s	0.96 s
OH-11				4.74 s					

[a]Chemical shifts (δ) downfield from TMS, J couplings (in parentheses) in Hz run at 400.13 MHz. [b]Assignments may be interchanged.

DOI: 10.1021/acs.jnatprod.8b00162
J. Nat. Prod. XXXX, XXX, XXX–XXX

Table 2. ^{13}C NMR Data of Compounds 1−9 in $CDCl_3$[a]

position	1	2	3	4	5	6	7	8	9
1	33.4	72.6	31.8	73.8	32.5	33.7	33.7	31.1	32.7
2	29.7	33.1	41.7	34.9	27.7	26.9	29.1	24.5	24.6
3	30.9	24.2	210.1	25.3	30.1	30.5	30.7	30.2	30.8
4	40.4	42.6	42.15	41.8	41.2	38.4	40.6	36.1	44.0
5	42.8	41.1	42.22	44.1	43.9	41.4	41.6	43.5	40.5
6	37.3	41.5	43.1	151.3	159.8	66.8	66.2	28.6	36.2
7	66.3	66.8	144.6	141.4	136.6	63.7	63.5	157.2	157.2
8	195.7	196.2	203.4	188.8	184.1	Nd	Nd	98.3	102.7
9	123.7	127.4	37.9	127.0	124.9	121.0	120.5	64.3	64.8
10	173.0	167.7	55.6	166.5	168.0	167.0	169.5	69.1	67.1
11	65.3	65.2	130.1	72.2	199.3	201.6	202.2	123.6	123.8
12	19.4	18.8	23.6	29.2a				171.9	171.9
13	21.8	21.2	22.6	29.3a	30.9	28.38	28.3	8.8	8.6
14	17.0	15.1	15.3	16.5	16.1	16.1	15.8	16.2	16.3
15	21.5	20.0	11.9	19.0	16.9	18.0	15.7	17.8	17.8

[a]Chemical shifts (δ) downfield from TMS; 100.03 MHz.

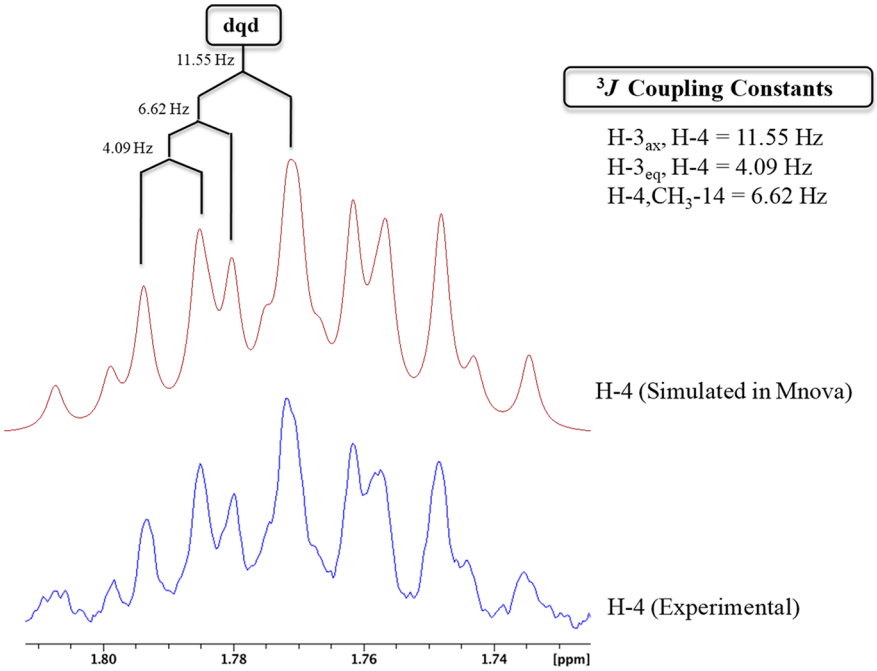

Figure 2. Multiplicity of the ^1H NMR signal of H-4 of compound **1** obtained by the spin system simulation plug-in in MNova using the experimental $^3J_{HH}$ extracted as described in the text. The signal is a dqd of 11.6, 6.6, and 4.1 Hz, respectively. Experimental (blue) and simulated (red).

module of MNova (simulated vs experimental multiplicity of the H-4 signal is shown in Figure 2) using a line width value of 1.5 Hz. An excellent match with the experimental data was obtained. The DQF-Phase Sensitive COSY of a 77.5:22.5 mixture of **1** and **13** showed a similar H-4 and CH_3-14 cross-peak intensity for both compounds (Figure 3), clear evidence that **1** and **13** share the same relative configuration at the C-4 and C-5 stereocenters. Consequently, the only difference between these two compounds should be the configuration of the 7,11-epoxy moiety. Assuming that the reported relative configuration of the epoxy moiety for **13** was correctly determined, we could infer that the only remaining option for the epoxy of **1** is the opposite configuration. The reported NOESY spectrum of **13** showed an NOE for CH_3-15 with CH_3-13 and CH_3-14.[9] For compound **1**, the NOE with CH_3-13 is absent. However, NOE enhancement in small molecules is often miniscule due to a poor efficiency of the dipole−dipole relaxation mechanism[12] therefore limiting the maximum distance at which an NOE can be observed. This led us to consider other powerful and modern techniques to accurately determine the relative configuration of both compounds.

The development of the application of Residual Dipolar Couplings (RDCs) to the configurational and conformational analysis of small molecules has matured in recent years.[13−15] Since RDCs provide information on nonlocal character they may allow the determination of the relative configuration of stereocenters when conventional NMR parameters such as NOE and ^3J coupling constants fail to provide an unambiguous solution.[16−18]

To obtain the experimental RDCs for compounds **1** and **13**, $^1H-^{13}C$ coupling constants were measured ($^1J_{CH}$) in F1-coupled HSQC experiments in isotropic and total coupling

DOI: 10.1021/acs.jnatprod.8b00162
J. Nat. Prod. XXXX, XXX, XXX−XXX

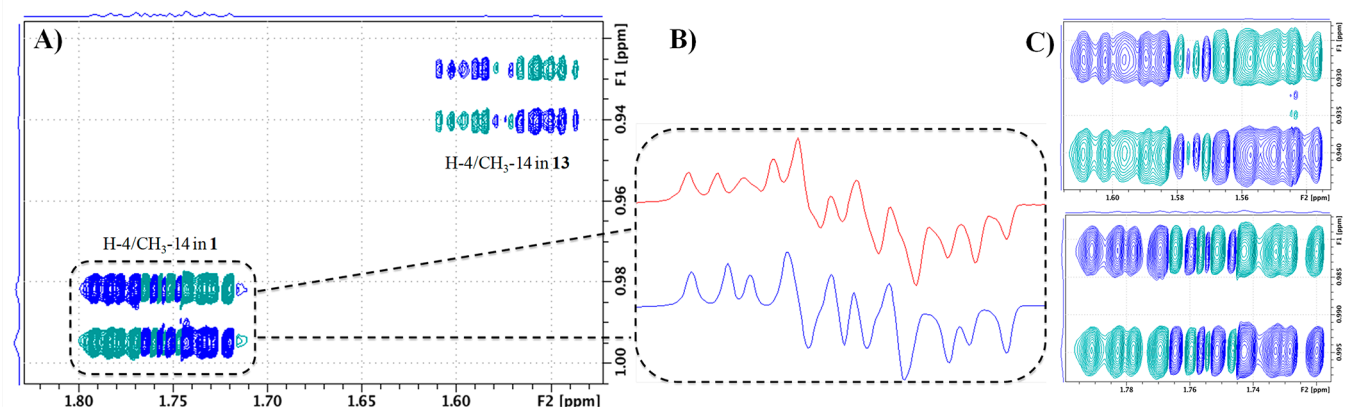

Figure 3. (A) Cross-peak H-4/CH_3-14 for compounds **1** and **13** in the DQF-PH-COSY spectrum of the mixture (different intensities are due to the difference in concentration), (B) H-4 F2 traces of cross-peak H-4/CH_3-14 in the DQF-PH−COSY spectrum of the mixture (**1**, major, in red and **13** in blue, minor), (C) Expansion of cross-peak H-4/CH_3-14 of isomers **1** (up, 1.76/0.99 ppm) and **13** (down, 1.57/0.94 ppm) mixture.

Table 3. Multi NMR Parameters Fitting for Compounds 1 and 13

		RDCs (for compound **13**)		RDCs + ^{13}C + ^{1}H (combined fitting for **13**)		RDCs (for compound **1**)		RDCs + ^{13}C + ^{1}H (combined fitting for **1**)	
		AIC	Rel. Prob. (%)	AIC	Rel. Prob. (%)	AIC	Rel. Prob. (%)	AIC	Rel. Prob. (%)
A	4*S*, 5*R*, 7*R*	0.5	9.9×10^{01}	41.1	1.7×10^{00}	0.7	1.0×10^{02}	33.8	1.0×10^{02}
B	4*S*, 5*R*, 7*S*	0.5	1.0×10^{02}	32.9	1.0×10^{02}	1.1	8.2×10^{01}	46.1	2.1×10^{-01}
C	4*R*,5*R*, 7*R*	2.6	3.5×10^{01}	71.0	5.4×10^{-07}	2.3	4.5×10^{01}	68.6	2.7×10^{-06}
D	4*R*, 5*R*, 7*S*	1.6	5.8×10^{01}	89.8	4.4×10^{-11}	3.9	2.0×10^{01}	83.8	1.4×10^{-09}

($^{1}T_{CH}$=$^{1}J_{CH}$+$^{1}D_{CH}$) in anisotropic media, for both molecules. Reversibly compressing poly methyl methacrylate (PMMA) gels compatible with $CDCl_3$ were used as an aligning media to induce anisotropy. These gels offer the additional advantage of easy recovery of the compound by dialyzing the gel after the RDC measurement.[19] In order to increase the measurement precision and facilitate the extraction of experimental RDCs, *J*-Scaled-BIRD-HSQC experiments with proton homonuclear decoupling (pure-shift) capabilities were used.[20] It was intriguing to observe that, although having the same molecular constitution, compound **1** poorly aligned (very small RDCs) compared to compound **13**, as shown in Table 3. The molecular modeling of these two compounds, as shown below, revealed interesting geometrical properties which explain this observation.

Using the recently published Computer Assisted 3D Structure Elucidation (CASE-3D) protocol,[21,22] the 2D structure (same for **1** and **13**) was fed into LigPrep/Maestro programs in order to automatically generate all possible configurations and respective conformational ensembles using the MMFF94 force field.[23] Since these structures have three stereogenic carbons, four possible diastereoisomers (Figure 4) were generated. The fact that **1** and **13** share the same configuration in ring A was ignored in order to avoid any bias in the determination of the correct structures of **1** and **13**. The conformational search was performed using molecular mechanics (MMFF94) of the geometry for all configurations.[24] (See Experimental Section and Supporting Information for computational details). Two major conformers were found for each diastereoisomer. These two conformations were called extended and folded, in which H-6β adopts an equatorial or axial position, respectively. As part of the CASE-3D protocol, ^{1}H and ^{13}C chemical shifts were calculated at the DFT B3LYP/6-31G* level followed by fitting the structures (configuration/conformations) to RDCs and experimental $^{1}H/^{13}C$ NMR chemical shifts using the Akaike information criterion (AIC) for model selection as implemented in StereoFitter.[25]

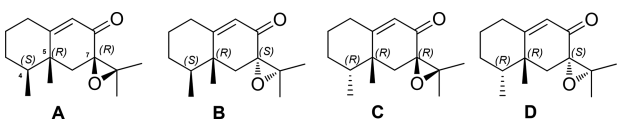

Figure 4. Possible diastereomers for structure of compounds **1** and **13**.

The four diastereomers were named using the *R*/*S* descriptors in place of the stereogenic carbon numbers in ascending order, e.g. 4*R*5*R*7*R* is named just as *RRR* (Figure 4).

Multi NMR parameters fitting (RDCs, $^{1}H/^{13}C$ chemical shifts) of the experimental data of compounds **1** and **13** to each ensemble of structures clearly ruled out the configurations *RRR* (**C**) and *RRS* (**D**) with very high AIC and low probability values, as shown in Table 3. The data of compound **1** had a clearly better fit for configurations *SRR* (**A**), while for compound **13** the multiparameter fitting indicated configuration *SRS* (**B**), as previously reported.[9]

As mentioned above, the conformational search found two conformers per diastereoisomer. The molecules show flexibility in the ring containing the epoxy group leading to a folded and extended form as shown in Figure 5. The fittings selected the folded form for compound **1** but the extended one for **13**, in agreement with the extended → folded energy differences ΔH_0 of −1.9 kcal/mol for **1** and 4.3 kcal/mol for **13** as revealed by the M062*X*/6-31+G** DFT calculations. These results may explain why compound **1** poorly aligns in PMMA/$CDCl_3$ gels compared to compound **13**. To the same degree of anisotropy provided by the alignment media, the degree of alignment of a

DOI: 10.1021/acs.jnatprod.8b00162
J. Nat. Prod. XXXX, XXX, XXX−XXX

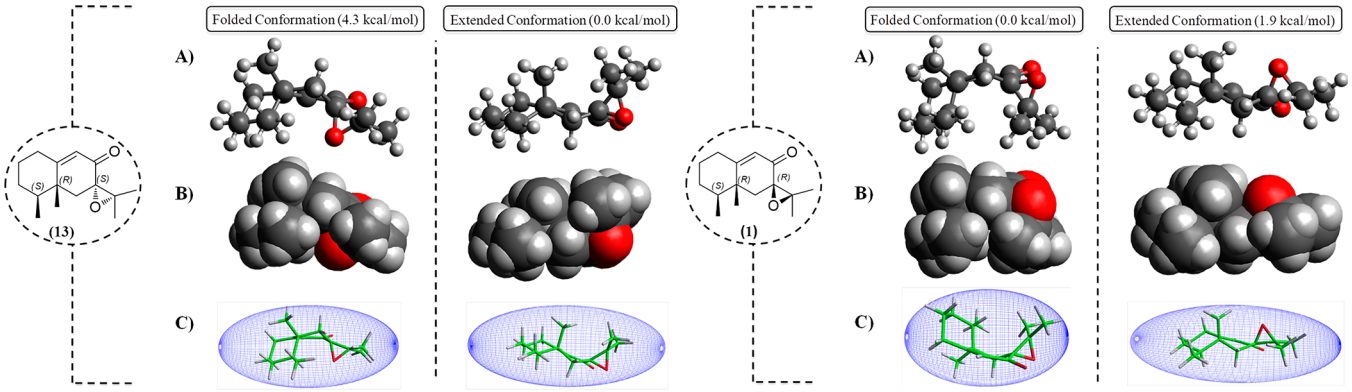

Figure 5. Lowest energy conformers for isomers **13** and **1**. Different representations of molecules to visualize molecular shapes and sizes produced by the flexibility of the epoxy group (A, ball and sticks; B, Van der Walls spheres; and C, gyration ellipsoids). Note the drastic change in anisotropy, more appreciable in extended form of isomer **13** with respect to the folded form of **1**, which explains the values of RDCs obtained for each compound (see text, page 8).

given molecule strongly depends on its size and shape. Very small and rounded in shape molecules poorly align, and in many cases the values of RDCs are very small and within the margin of error. Compared to compound **13**, compound **1** shows small $^{1}D_{CH}$ RDCs. This is now clearly explained by the almost globular shape adopted by the lowest energy conformation of compound **1** (folded form) that is much less anisotropic than the extended form of compound **13**, explaining why **13** shows larger RDC values than **1** (see gyration ellipsoids in Figure 5).[26] These results also agree with the observation of an NOE peak between CH_3-15 and CH_3-13 in **13** but not in **1**. In compound **1** the CH_3-13/CH_3-15 interproton distances are over 5.0 Å whereas in **13** they can be as small as ~2.6 Å, explaining the observation of an NOE peak. In summary, the structure of **1** was elucidated as rel-(4*S*,5*R*)-7*β*,11*β*-epoxyeremophil-9-en-8-one.

Compound **2** could not be obtained in pure form by normal or reversed-phase TLC. Consequently, it was characterized from 2.2 mg of a mixture of compounds **2** and **16** in a 3:2 ratio. Compound **2** revealed a molecular formula of $C_{15}H_{22}O_3$ by UPLC-HRMS, with the ^{1}H and ^{13}C NMR data (Tables 1 and 2) being closely comparable to those of compounds **1** and **13**. The only difference between **2** and the isomers **1** and **13** was the presence of signals corresponding to the oxygenated methine assigned at C-1 (δ_H 4.35 brs and δ_C 72.6) in **2**. The hydroxy group was located at C-1 by the HMBC correlations between the signals of H-1 and C-3 (δ 24.2), C-5 (δ 41.1), and C-9 (δ 127.4) (Figure S2–4, Supporting Information). The *β* orientation of the hydroxy group at C-1 was established by the analysis of the coupling constant (brs) and confirmed by the NOE observed between H-1 and H-4 at δ 1.48 m and H-9 at δ 5.91 (Figure S2–5, Supporting Information), while the NOEs observed were inconclusive to determine the orientation of the epoxy group. A CASE-3D $^{13}C/^{1}H$ chemical shifts study selected an *α*-orientation of the epoxy group (Table 4), with relative probabilities between the two closest forms of ~1% when using the ^{13}C chemical shifts data alone and ~0.1% when using both ^{1}H and ^{13}C chemical shift data. Accordingly, compound **2** was characterized as rel-(4*S*,5*R*)-1*β*-hydroxy-7*α*,11a-epoxyeremophil-9-en-8-one.

Compound **3** revealed a molecular formula of $C_{15}H_{22}O_2$, as determined by HRESIMS. The ^{1}H NMR data of **3** showed four methyl signals at δ 2.01 (d, J = 2.2 Hz), 1.79 (d, J = 1.4 Hz), 1.02 (d, J = 6.6 Hz), and 0.7 s (Table 1). The resonances

Table 4. Multi NMR Parameters Fitting for Compound 2

		^{13}C (for compound **2**)		^{13}C + ^{1}H (combined fitting for **2**)	
		AIC	Rel. Prob. (%)	AIC	Rel. Prob. (%)
A	1*R*,4*S*,5*R*,7*R*	28.4	1.1×10^{00}	57.5	4.4×10^{-01}
B	1*R*,4*S*,5*R*,7*S*	19.4	1.0×10^{02}	46.7	1.0×10^{02}
C	1*S*,4*S*,5*R*,7*R*	44.7	3.3×10^{-04}	77.1	2.5×10^{-05}
D	1*S*,4*S*,5*R*,7*S*	36.5	1.9×10^{-02}	63.8	2.0×10^{-02}
E	1*R*,4*S*,5*S*,7*R*	43.7	5.4×10^{-04}	73.3	1.7×10^{-04}
F	1*R*,4*S*,5*S*,7*S*	54.3	2.6×10^{-06}	82.1	2.1×10^{-06}
G	1*S*,4*S*,5*S*,7*R*	41.4	1.7×10^{-03}	82.3	1.9×10^{-06}
H	1*S*,4*S*,5*S*,7*S*	56.8	7.4×10^{-07}	95.7	2.3×10^{-09}

at δ 2.01 and δ 1.79 are typical of methyl groups bonded to vinylic carbons. Inspection of the 1D and 2D NMR spectroscopic data suggested that compound **3** had similar signals for all carbons and protons as fukinone.[27] The main difference observed between fukinone and compound **3** was the signal corresponding to a carbonyl group at δ 210.0 assigned at C-3. The position of the carbonyl group was confirmed through the analysis of the COSY, HSQC, and HMBC spectra. A detailed examination of the COSY spectrum of compound **3** led to establishment of three spin systems: an $A_2B_2CD_2$ system consisting of H_2-2 (δ 2.41 m), H_2-1 (δ 1.94 and 1.69 m), H-10 (δ 2.72, dd, J = 12.6,4.2 Hz), and H_2-9 (δ 2.64 and 2.40 m), an AB_3 system consisting of H-4 (δ 1.90 m) and H_3-14, and an $A_2B_3C_3$ consisting of H_2-6 [δ 2.79 (d, 14.8 Hz) and 2.12 (d, 14.8 Hz)], H_3-12, and H_3-13, respectively (Figure S3-3, Supporting Information). The *β* orientation of the proton at C-10 (*cis* decalin) was determined by the multiplicity and the coupling constant value of H-10 [δ 2.72 (dd, J = 12.6, 4.2 Hz)] (Figure S3-6, Supporting Information). Thus, the structure of compound **3** was established as rel-(4*R*,5*S*,10*R*)-eremophil-7(11)-en-3,8-dione.

The molecular formula of compound **4** was determined by HRESIMS as $C_{15}H_{22}O_3$. Its ^{1}H and ^{13}C NMR spectra were closely related to those of 11-hydroxyeremophil-6,9-dien-8-one (**15**), previously isolated from *Senecio desfontainei*,[28] differing only in the substitution pattern of ring A (Tables 1 and 2). The NMR spectroscopic data of compound **4** suggested the presence of a hydroxy group at C-1 [δ_H 4.46 (t, J = 2.6 Hz), δ_C 73.8]. The location of this group was supported by the HMBC cross-peaks of the signals of H-1, with C-3 (δ 25.3), C-

DOI: 10.1021/acs.jnatprod.8b00162
J. Nat. Prod. XXXX, XXX, XXX−XXX

Table 5. Multi NMR Parameters Fitting for Compounds 6 and 7

		^{13}C (for compound **6**)		^{13}C + ^{1}H (combined fitting for **6**)		^{13}C (for compound **7**)		^{13}C + ^{1}H (combined fitting for **7**)	
		AIC	Rel. Prob.(%)	AIC	Rel. Prob.(%)	AIC	Rel. Prob.(%)	AIC	Rel. Prob.(%)
A	4*S*,5*R*,7*R*,8*R*	**14.6**	**1.0 × 10^{02}**	**28.8**	**9.7 × 10^{01}**	22.9	4.4 × 10^{01}	47.1	3.8 × 10^{-02}
B	4*S*,5*R*,7*S*,8*S*	18.4	1.5 × 10^{01}	28.8	1.00 × 10^{02}	**21.2**	**1.0 × 10^{02}**	**31.4**	**1.0 + 02**
C	4*S*,5*S*,7*R*,8*R*	38.3	7.0 × 10^{-04}	62.7	4.4 × 10^{-06}	55.7	3.2 × 10^{-06}	82.0	1.0 × 10^{-9}
D	4*S*,5*S*,7*S*,8*S*	53.2	4.0 × 10^{-07}	67.4	4.2 × 10^{-07}	78.2	4.2 × 10^{-11}	94.8	1.7 × 10^{-12}

Table 6. Multi NMR Parameters Fitting for Compounds 8 and 9 Data

		^{13}C (for compound **8** data)		^{13}C + ^{1}H (combined fitting for **8** data)		^{13}C (for compound **9** data)		^{13}C + ^{1}H (combined fitting for **9** data)	
		AIC	Rel. Prob.(%)	AIC	Rel. Prob.(%)	AIC	Rel. Prob.(%)	AIC	Rel. Prob. (%)
A	4*S*,5*R*,8*R*,9*R*,10*R*	12.2	1.0 × 10^{02}	44.2	1.0 × 10^{02}	59.4	5.8 × 10^{-08}	94.7	8.9 × 10^{-10}
B	4*S*,5*R*,8*S*,9*R*,10*R*	44.7	8.4 × 10^{-06}	93.5	2.0 × 10^{-09}	16.9	1.0 × 10^{02}	43.8	1.0 × 10^{02}
C	4*S*,5*R*,8*R*,9*S*,10*S*	62.0	1.5 × 10^{-09}	124.7	3.3 × 10^{-16}	36.5	5.4 × 10^{-03}	83.2	2.8 × 10^{-07}
D	4*S*,5*R*,8*S*,9*S*,10*S*	22.7	5.0 × 10^{-01}	93.4	2.0 × 10^{-09}	44.7	8.8 × 10^{-05}	85.7	7.8 × 10^{-08}
E	4*S*,5*S*,8*R*,9*R*,10*R*	42.9	2.1 × 10^{-05}	102.5	2.1 × 10^{-11}	71.4	1.5 × 10^{-10}	117.6	9.5 × 10^{-15}
F	4*S*,5*S*,8*S*,9*R*,10*R*	80.7	1.3 × 10^{-13}	160.5	5.5 × 10^{-24}	83.6	3.2 × 10^{-13}	151.1	5.0 × 10^{-22}
G	4*S*,5*S*,8*R*,9*S*,10*S*	40.5	6.9 × 10^{-05}	91.9	4.3 × 10^{-09}	54.3	7.4 × 10^{-07}	88.8	1.7 × 10^{-08}
H	4*S*,5*S*,8*S*,9*S*,10*S*	39.9	9.6 × 10^{-05}	80.7	1.2 × 10^{-06}	44.6	9.5 × 10^{-05}	79.7	1.6 × 10^{-06}

5 (44.1), and C-9 (127.0), and by the allylic coupling between H-1 and H-9 in the COSY spectrum (Figures S4-5 and S4-3, Supporting Information). The β orientation of the hydroxy group at C-1 was established based on the coupling constant between H-1 and H_2-2 (t, J = 2.6 Hz) and confirmed by the NOE observed between H-1 and H-4 at δ 1.51 m (Figure S4-6, Supporting Information). Thus, the structure of compound **4** was established as rel-(4*S*,5*S*)-1β,11-dihydroxyeremophil-6,9-dien-8-one. Ruiz-Vásquez et al. reported a constituent of *Senecio adenotrichius* with the same structure as **4**, but it was inconsistent with the reported spectroscopic data.[29] The reported chemical shift for C-11 (δ 83.5) agreed with the presence of a hydroperoxy group at C-11 but not with a hydroxy group.[30]

The molecular formula of compound **5** was determined by HRESIMS as $C_{14}H_{18}O_2$, indicating that **5** is a nor-sesquiterpenoid. Except for the absence of signals corresponding to a hydroxy group, the ^{1}H and ^{13}C NMR signals of **5** (Tables 1 and 2) were nearly superimposable with those of 3β-hydroxy-11-noreremophila-6,9-diene-8,11-dione isolated from *Ligularia japonica*,[31] indicating that they share the same sesquiterpenoid skeleton. Thus, the structure of **5** was elucidated as rel-(4*S*,5*S*)-11-noreremophila-6,9-diene-8,11-dione.

Compounds **6** and **7** could not be obtained in pure form by normal or reversed-phase TLC. Consequently, these compounds were characterized from 3 mg of a **6**/**7** 3:2 ratio mixture. The molecular formula of the mixture of **6** and **7** was unambiguously determined by UPLC-HRMS as $C_{14}H_{18}O_2$, indicating that **6** and **7** are nor-sesquiterpenoid isomers. The ^{1}H and ^{13}C NMR spectra of **6** were related to those of **5** (Tables 1 and 2). The resonances from ring A and the substituent at C-7 were similar to those in compound **5**, indicating that structural differences between these two nor-sesquiterpenoids were restricted to ring B. In addition to the presence of an α,β-unsaturated carbonyl function in ring B [δ_H 5.71 (d, J = 1.8 Hz, H-9), δ_C 121.0 (C-9), and δ_C 167.0 (C-10)], an epoxy group was evident in the ^{1}H NMR spectrum from the singlet at δ 3.42 corresponding to H-6, in agreement with the signals at δ 66.8 and 63.7 in the ^{13}C NMR spectrum. The location of the 6,7-epoxy group was confirmed by the cross-correlation peaks of H-6, with C-5 (δ 41.4), C-10 (167.0), and C-15 (18.0) in the HMBC spectrum (Figure S6–4, Supporting Information). The orientation of the epoxy group was established from a NOESY correlation observed for H-6 with CH_3-15 at δ 1.15 indicating the α orientation (Figure S6–5, Supporting Information). The ^{1}H and ^{13}C NMR data of isomer **7** were highly similar to those of compound **6**, differing only in the orientation of the 6,7-epoxy group. On the basis of CASE-3D ^{13}C and ^{1}H chemical shift analyses the structures were assigned as rel-(4*S*,5*R*)-6α,7α-epoxy-11-noreremophila-9-en-8,11-dione and rel-(4*S*,5*R*)-6β,7β-epoxy-11-noreremophila-9-en-8,11-dione (Table 5).

Finally, compounds **8** and **9** could also not be obtained in pure form by normal or reverse phase TLC; they were therefore characterized from 2.2 mg of a 5:2 mixture. The molecular formula of these components was determined by UPLC-HRMS as $C_{15}H_{20}O_4$, indicating that **8** and **9** were also isomers. The ^{1}H NMR spectrum of **8** exhibited only three signals corresponding to methyl groups at δ 1.74 (d, J = 0.8 Hz), 0.87 (d, J = 6.8 Hz), and 1.07 s, assigned to H_3-13, H_3-14, and H_3-15 of an eremophilane lactone similar to compound **16** isolated from *S. rosmarinus*.[8] The presence of an unsaturated lactone hydroxylated at C-8 was confirmed by the signals at δ 157.2, 98.3, 123.6, 171.9, and 8.8 in the ^{13}C NMR spectrum (Table 2), which were assigned to C-7, C-8, C-11, C-12, and C-13, respectively. Furthermore, a singlet at δ 3.27 in the ^{1}H NMR spectrum and the resonances at δ 64.3 and 69.1 in the ^{13}C NMR spectrum were consistent with the presence of the epoxy group. The position of this group at C-9 and C-10 was established by the HMBC correlation between the H-9 and C-1 at δ 31.1, C-8 at 98.3, and C-7 at 157.2 (Figure S7–5, Supporting Information). The orientations of the 8β-hydroxy and 9β,10β-epoxy groups were determined on the basis of the NOEs observed between H_3-15 and the signals corresponding to H-6a at δ 2.43 (d, J = 13.0 Hz) and H-6b at 2.11 (brd, J = 13.0 Hz) in the NOESY experiment (Figure S7–6, Supporting Information). The highly similar NMR data for compounds **8**

DOI: 10.1021/acs.jnatprod.8b00162
J. Nat. Prod. XXXX, XXX, XXX−XXX

and **9** (Tables 1 and 2) indicated that structural differences were restricted to the orientation of the hydroxy group at C-8 and/or the epoxy group at C-9 and C-10. For compound **9**, the α orientation of the 8-hydroxy group was confirmed by the correlation peak observed between H_3-13 at δ 1.73 and the resonance corresponding to H_3-15 at 0.96 (Figure S7−7, Supporting Information), while the orientation of the epoxy group could not be confirmed on the basis of the observed NOEs. Therefore, a CASE-3D chemical analysis, analogous to the one used for **1** and **2**, but only on the basis of ^{13}C and ^{1}H DFT predicted chemical shifts was performed. Fitting the ^{13}C NMR chemical shift data alone selected the configurations of **8** and **9** as rel-(4*S*,5*R*)-9β,10β-epoxy-8β-hydroxy eremophil-12,8-olide and rel-(4*S*,5*R*)- 9β,10β-epoxy-8α-hydroxy eremophil-12,8-olide, respectively, with more than a 100:1 relative probability (Table 6). Adding ^{1}H NMR chemical shifts to the fitting resulted in much increased selection capability (relative probability less than 10^{-3}%).

Considering the biological activity shown by several eremophilans,[39,40] the in vitro antiproliferative activities of sesquiterpenoids **1**, **2**, **5**, **10**, **11**, **12**, **14**, **15**, and **16** were evaluated using the well-established protocol of the National Cancer Institute (NCI) of the United States.[41] As a model, the representative panel of human solid tumor cell lines A549 (lung), HBL-100 (breast), HeLa (cervix), SW1573 (nonsmall cell lung), T-47D (breast), and WiDr (colon) was used. All compounds tested showed GI_{50} > 10 μM (Sections S8-1 and S8-2, Supporting Information).

In addition to the nine new compounds (**1**−**9**), six known sesquiterpenoids (**10**−**16**) and 4-hydroxyacetophenone (**17**) were also isolated and identified by comparison with published spectroscopic and physical data as 1α-hydroxy and 1β-hydroxy dehydrofukinones (**10**, **11**),[32] dehydrofukinone (**12**),[33] ligudicins A and C (**13**, **14**),[9] 11-hydroxyeremophil-6,9-dien-8-one (**15**),[27] and istanbulin A (**16**).[34] The presence of 4-hydroxyacetophenone and derivatives has been reported in several *Senecio* species.[29,35,36]

The occurrence of pyrrolizidine alkaloids has been reported in most *Senecio* species. For this reason, 200 gr of the aerial part of *S. volckmannii* was processed using a specific methodology for their extraction.[37] This extract was analyzed by ^{1}H NMR and CG/MS, and surprisingly, no pyrrolizidine alkaloids were observed. In other *Senecio* species, such as *S. chionophilus*, the absence of alkaloids has also been reported.[38]

The major components obtained in this work are eremophilanes, metabolites widely distributed in nature, reported from endophytic fungus such as Xylariaceous microorganism as well as in higher plants.[4,5] Numerous eremophilane-type sesquiterpenoids have been reported, not only in the genera *Senecio* but also in *Ligularia* species, among others. Through a combination of NMR tools such as $^{3}J_{HH}$ coupling constant analysis, spin systems simulations, DQF-Phase Sensitive COSY, Computer Assisted 3D Structure Elucidation (CASE-3D) using DFT predicted ^{1}H/^{13}C chemical shifts, and RDCs, the configuration of the new compound **1** was unequivocally determined. The structural resolution (behavior of isomers **1** and **13**) permitted an investigating about differential ordering in very small molecules in alignment media, where the analysis of molecular shape,[26] through for instance visualization of the gyration tensor, is decisive. Computer Assisted 3D Structure Elucidation (CASE-3D) using DFT predicted ^{1}H/^{13}C chemical shifts permitted the characterization of compounds **2** and **6**−**9**, which were isolated as mixtures.

EXPERIMENTAL SECTION

General Experimental Procedures. Optical rotations were measured on a JASCO P-1010 polarimeter or on a JASCO J-810 spectropolarimeter (as ORD measurements). The UV spectra were obtained using a Shimadzu-260 spectrophotometer, and IR spectra were produced using a Thermo Scientific Nicolet iN10 FT-IR Microscope. NMR spectra were recorded on a Bruker AVANCE II AV-400 operating at 400.13 MHz for ^{1}H and 100.63 MHz for ^{13}C, while 2D spectra (COSY, HSQC, HMBC, and NOESY) were obtained using standard Bruker software. Chemical shifts are given in ppm (δ) downfield from the TMS internal standard. RDC measurements were recorded on a Bruker AVANCE III NMR spectrometer, operating at 500.13 MHz for ^{1}H, 125.76 MHz for ^{13}C, and 76.77 MHz for ^{2}H. One-bond proton-carbon residual dipolar couplings ($^{1}D_{CH}$) were measured with the F1 proton coupled *J*-scaled BIRD HSQC experiment,[42] as from the Bruker pulse sequence library, using a *J*-scaling factor (κ) of 4 and INEPT transfer optimized for a 145 Hz ^{1}H−^{13}C coupling constant. A total of 1024 increments in F1 were used. Anisotropic conditions were obtained using cross-linked PMMA gels swollen in $CDCl_3$ using the reversible compression/relaxation method as described previously.[19] PMMA Gels, Compression Devices, and the StereoFitter program are commercially available from Mestrelab Research.

HRESIQTOFMS were determined on a Micro TOF II Bruker Daltonics (MA, USA). UPLC-ESI-QTOF/MS was performed using a system: UPLC equipment Agilent Technologies 1200 LC (Agilent, Santa Clara, CA, USA) coupled to a PDA detector (Agilent Series 1200) in tandem with an ESI source, operated in positive mode connected to a MicroQTOF II (Bruker Daltonics, Billerica, MA, USA) mass spectrometer (MS). The UPLC system was equipped with a binary pump, solvent degasser, and autosampler (Agilent Series 1200 L, Santa Clara, CA, USA). UPLC analyses were performed on a Phenomenex column (C_{18}, 100 × 2.10 mm, 2.6 μm) at 35 °C and 0.25 mL/min flow rate, using an isocratic mixture of acetonitrile and water 60:40. Chromatographic separations were performed by column chromatography on silica gel 60 (0.063−0.200 mm) and Sephadex LH-20, radial chromatography with a radial Chromatotron Model 7924 T on silica gel 60 PF_{254} Merck (1 mm thick), and preparative TLC on silica gel 60 F_{254} (0.2 mm thick) plates. Preparative TLC separations were performed under the following conditions: (i) the amount of sample applied was approximately 15 mg for 20 cm plate; (ii) the bands were visualized using ultraviolet light; (iii) compounds were eluted from the silica using CH_2Cl_2:MeOH (8:2). RP-HPLC separations were achieved on a DIONEX Ultimate 3000 apparatus equipped with an Agilent column (ZORBAX Eclipse XDB-C_{18}, 4.6 × 250 mm, 5-μm) and a DIONEX Ultimate 3000 variable wavelength detector fixed at 250 nm. Chromatographic/Mass Spectrometer analyses were carried out on a Shimadzu GC/MS QP-5050 spectrometer equipped with VF-5 ms, 30 m x 0.25 mm x 0.25 μm column.

Computational Procedures. Geometries for all diastereoisomeric forms of **1**, **2**, **8**, **9**, and **13** were generated using the Schrödinger Ligprep program[43] and conformational spaces explored determined using the MMFF94 force field[44] and the MonteCarlo Multiple minimum algorithm[45] in Macromodel.[46] The conformations below a threshold of 21 kJ/mol were kept.

^{1}H and ^{13}C NMR chemical shieldings were computed at the GIAO/B3LYP 6-31G* level in Gaussian09. Conformations of **1** were refined *in vacuo* at the M062*X*/6-31+G** level of theory using the "ultrafine" Gaussian09[24] grid. Harmonic vibrational frequencies were computed at the same level of theory and verified to be minima in the potential surface. The experimental RDCs and chemical shifts were fitted to the conformational ensembles using the recently described procedure implemented in the StereoFitter program.[21] In this procedure the best scoring conformational model for each particular configuration was obtained through minimizing quadratic differences

DOI: 10.1021/acs.jnatprod.8b00162
J. Nat. Prod. XXXX, XXX, XXX−XXX

(χ^2) between experimental and computed RDCs and chemical shift data. Overfitting is avoided by using the Akaike information criterion (AIC) for model selection. Configurations are then ranked according to their AIC differences. These differences can be interpreted in terms of probabilities defined as $\frac{p_i}{p_{min}} = e^{-(AIC_i - AIC_{min})/2.0}$ where p_i/p_{min} is the relative probability of the best model for the ith configuration to recover the lost information with respect to that for the best-scoring configuration. During the fitting procedure chemical shieldings were transformed into chemical shifts by using a linear relationship $\delta = a\varsigma +$ b where slope a and intercept b were obtained by fitting ^{1}H and ^{13}C NMR experimental chemical shifts of β-pinene to compute shieldings at exactly the same level of theory.[47] RDCs and chemical shifts were weighted in the fitting procedure using standard errors for ^{1}H and ^{13}C shifts of 0.15 and 2 ppm whereas RDCs were weighted by a standard error of 1.2 Hz. Additionally RDCs and chemical shifts from diastereotopic protons and epoxy methyl groups were averaged during the fitting procedure in order to avoid a priori assignment of these groups.

Plant Material. The aerial parts of *Senecio volckmannii* Phil. plants were collected at 3500 m above sea level at the Vinchina Department, La Rioja, Argentina, in February 2001. A voucher specimen was deposited at the Museo Botánico Córdoba, Universidad Nacional de Córdoba (CORD 40584). The plant material was identified by Gloria E. Barboza (IMBIV-CONICET, Córdoba, Argentina).

Extraction and Isolation. The dry and pulverized aerial parts of *S. volckmannii* (250 g) were extracted successively with *n*-hexane and CH_2Cl_2 (3 × 500 mL). The CH_2Cl_2 extract was dried over anhydrous Na_2SO_4, filtered, and evaporated to dryness at reduced pressure. The residue (6.00 g) was chromatographed initially on a Sephadex LH-20 column, using MeOH as eluent. Fractions with similar TLC profiles were combined and reduced to four fractions (I–IV), with fraction II containing sesquiterpenoids and fraction III containing 4-hydroxyacetophenone (**17**) (200 mg). Fraction II was further chromatographed on silica gel 60 G CC. Elution with *n*-hexane–EtOAc mixtures of increasing polarity (100:00 to 0:100) afforded six fractions (I–VI). Of these, fraction I was the known sesquiterpenoid dehydrofukinone (**12**) (321.5 mg). Fraction II (62.0 mg) was purified by preparative TLC with CH_2Cl_2/MeOH (99.7:0.3) to obtain two subfractions (I1 and I2). These subfractions were fractionated by reverse-phase HPLC and eluted with an isocratic mixture of MeCN/H_2O (60:40) at 1 mL/min flow rate. Subfraction I1 yielded compound **14** (2.4 mg), while subfraction I2 yielded compound **5** (2.5 mg) and a mixture (3.0 mg), which could not be separated by either normal phase TLC or reversed phase TLC. The ^{1}H NMR spectrum of this mixture indicated that it consisted of compounds **6** and **7** in a 3:2 ratio. Fraction III (42.4 mg) was processed by reverse-phase HPLC to obtain compound **15** (21.0 mg), and two fractions which were purified by preparative TLC with CH_2Cl_2/MeOH (99.0:1.0) to yield compounds **1** (8.1 mg) and **13** (2.6 mg), respectively. Fraction IV (59.5 mg) was separated by preparative TLC with CH_2Cl_2/MeOH (99.0:01.00) to obtain compounds **15** (16.7 mg) and **3** (7.5 mg). Fraction V (88.8 mg) was subjected to preparative TLC with CH_2Cl_2/MeOH (99.4:0.6) to afford compound **10** (5.0 mg). Finally, fraction VI (477.6 mg) was fractionated by radial chromatography with CH_2Cl_2–MeOH mixtures of increasing polarity (100:00 to 90:10) yielding two subfractions (VI1 and VI2). These subfractions were subjected to silica gel 60 G CC using CH_2Cl_2:MeOH mixtures of increasing polarity (100:0–80:20) to give compounds **5** (0.7 mg) and **11** (1.5 mg) from subfraction VI1 and two impure fractions from the subfraction VI2, which were rechromatographed by reverse-phase HPLC to yield compounds **4** (2.8 mg), **16** (1.6 mg), and two mixtures which could not be obtained pure by either normal phase TLC or reversed phase TLC: compounds **16** and **2** in a 3:2 ratio (2.2 mg) and compounds **8** and **9** in a 5:2 ratio (2.9 mg). The search for pyrrolizidine alkaloids was carried out using the Segall procedure over 200 g of sample.[37]

Rel-[(4*S*,5*R*)-7β,11β-epoxyeremophil-9-en-8-one] (**1**): White amorphous powder; $[\alpha]D^{21}$ −24 (*c* 0.2, $CHCl_3$), λ_{max} (log ε) 256.3 (3.23), 205.2 (3.15); IR (dry film) ν_{max} 3003, 2924, 2856, 1718, 16822, 1626 cm^{-1}; ^{1}H and ^{13}C NMR data, see Tables 1 and 2; HRESIMS *m*/*z* [M + Na]$^+$ 235.1697 (calcd for $C_{15}H_{23}NaO_2$, 235.1693).

Rel-[(4*S*,5*R*)-1β-hydroxy-7α,11α-epoxyeremophil-9-en-8-one] (**2**): White amorphous powder; ^{1}H and ^{13}C NMR data, see Tables 1 and 2; HRESIMS *m*/*z* [M + Na]$^+$ 273.1443 (calcd for $C_{15}H_{22}NaO_3$, 273.1461).

Rel-[(4*R*,5*S*,10*R*)-eremophil-7(11)-en-3,8-dione] (**3**): white amorphous powder; $[\alpha]_{270}{}^{21}$ −2 (*c* 0.1, $CHCl_3$); UV (CH_3OH) λ_{max} (log ε) 247.5 (3.34) nm, 206.0 (3.35) nm; IR (dry film) ν_{max} 2963, 2927.54, 2870, 1712, 1682 cm^{-1}; ^{1}H and ^{13}C NMR data, see Tables 1 and 2; HRESIMS *m*/*z* [M + Na]$^+$ 257.1502 (calcd for $C_{15}H_{22}NaO_2$, 257.1512).

Rel-[(4*S*,5*S*)-1β,11-dihydroxyeremophil-6,9-dien-8-one] (**4**): White amorphous powder; $[\alpha]_D{}^{21}$ −7 (*c* 0.3, $CHCl_3$); λ_{max} (log ε) 243.5 (3.40) nm, 206 (3.38) nm; IR (dry film) ν_{max} 3356, 2928, 2856, 1740, 1660, 1616 cm^{-1}; ^{1}H and ^{13}C NMR data, see Tables 1 and 2; HRESIMS *m*/*z* [M + Na]$^+$ 273.1458 (calcd for $C_{15}H_{22}NaO_3$, 273.1462).

Rel-[(4*S*,5*S*)-11-noreremophila-6,9-diene-8,11-dione] (**5**): White amorphous powder; $[\alpha]_{270}{}^{21}$ −9 (*c* 0.03, $CHCl_3$); λ_{max} (log ε) 243.50 (3.86) nm, 234.50 (3.86) nm, 212.50 (4.00) nm; IR (dry film) ν_{max} 2928, 2858, 2360, 2339, 1696, 1658 cm^{-1}; ^{1}H and ^{13}C NMR data, see Tables 1 and 2; HRESIMS *m*/*z* [M + Na]$^+$ 241.1206 (calcd for $C_{14}H_{18}NaO_2$, 241.1199).

Rel-[(4*S*,5*R*)-6α,7α-epoxy-11-noreremophila-9-en-8,11-dione] (**6**): White amorphous powder; ^{1}H and ^{13}C NMR data, see Tables 1 and 2; HRESIMS *m*/*z* [M + Na]$^+$ 257.1129 (calcd for $C_{14}H_{18}NaO_3$, 257.1148).

Rel-[(4*S*,5*R*)-6β,7β-epoxy-11-noreremophila-9-en-8,11-dione] (**7**): White amorphous powder; ^{1}H and ^{13}C NMR data, see Tables 1 and 2; HRESIMS *m*/*z* [M + Na]$^+$ 235.1319 (calcd for $C_{14}H_{19}O_3$, 235.1329).

Rel-[(4*S*,5*R*)-9β,10β-epoxy-8β-hydroxy-eremophil-12,8-olide] (**8**): White amorphous powder; ^{1}H and ^{13}C NMR data, see Tables 1 and 2; HRESIMS *m*/*z* [M + Na]$^+$ 287.1239 (calcd for $C_{15}H_{20}NaO_4$, 287.1254).

Rel-[(4*S*,5*R*)-9β,10β-epoxy-8α-hydroxy-eremophil-12,8-olide] (**9**): White amorphous powder; ^{1}H and ^{13}C NMR data, see Tables 1 and 2; HRESIMS *m*/*z* [M + Na]$^+$ 287.1235 (calcd for $C_{15}H_{20}NaO_4$, 287.1254).

■ ASSOCIATED CONTENT

Supporting Information

The Supporting Information is available free of charge on the ACS Publications website at DOI: 10.1021/acs.jnatprod.8b00162.

^{1}H NMR, COSY, HSQC-DEPT, and HMBC of compounds **1**, **2**, **4**, and **5**, and the mixtures of compounds **2**/**16**, **6**/**7**, and **8**/**9**. ^{13}C NMR of compounds **1** and the mixtures of compounds **2**/**16** and **8**/**9**. The relevant NOE correlations of compounds **2**, **4**, **6**, **8**, and **9**. The minimized structure of compound **3** (*cis*- and *trans*- decaline) (PDF)

A zip file with all computed structures, RDCs, and StereoFitter inputs and outputs (ZIP)

■ AUTHOR INFORMATION

Corresponding Authors

*Tel:/Fax: +54-351-535-3864. E-mail: manuelagarcia@fcq.unc.edu.ar.

*Tel:/Fax: +54-351-535-3864. E-mail: vnicotra@fcq.unc.edu.ar.

ORCID

Sebastián J. Castro: 0000-0001-5342-6660

Armando Navarro-Vázquez: 0000-0003-4364-516X

DOI: 10.1021/acs.jnatprod.8b00162
J. Nat. Prod. XXXX, XXX, XXX–XXX

Roberto R. Gil: 0000-0002-8810-5047
Viviana E. Nicotra: 0000-0002-5255-4721

Notes

The authors declare no competing financial interest.

■ ACKNOWLEDGMENTS

This work was supported by grants from CONICET (PIP 2012-2014, Res. 1675/12), SeCyT-UNC. S.J.C. thanks SeCyT-UNC (Argentina) for a fellowship. We thank G. E. Barboza (IMBIV-CONICET) for the collection and identification of plant material, G. Bonetto for NMR assistance, and J. Heywood, native speaker, for revision of this manuscript.

■ REFERENCES

(1) Freire, S. E.; Ariza Espinar, L.; Salomón, L.; Hernández, M. P.; Zuloaga, F. O.; Belgrano, M. J.; Anton, A. M. *Flora Argentina* **2014**, *7* (3), 27−220. IBODA-IMBIV, San Isidro.
(2) Romo de Vivar, A.; Pérez-Castorena, A.-L.; Arciniegas, A.; Villaseñor, J. L. *J. Mex. Chem.* **2007**, *51*, 160−172.
(3) Wiedenfeld, H.; Edgar, J. *Phytochem. Rev.* **2011**, *10*, 137−151.
(4) Fraga, B. M. *Nat. Prod. Rep.* **2011**, *28*, 1580−1610.
(5) Yang, Y.; Zhao, L.; Wang, Y. F.; Chang, M. L.; Huo, C. H.; Gu, Y. C.; Shi, Q. W.; Kiyota, H. *Chem. Biodiversity* **2011**, *8*, 13−72.
(6) Ariza Espinar, L. *Pródr. Fl. Fanerog. Argentina Central* **2010**, *6*, 3−71.
(7) Tortosa, R. D.; Bartoli, A. *Bol. Soc. Argent. Bot.* **2006**, *41*, 123−125.
(8) Morales, B. G.; Bórquez, R. J.; Mancilla, P. A.; Pedreros, T. S.; Loyola, L. A. *Phytochemistry* **1986**, *25*, 2412−2414.
(9) Tan, A. M.; He, H. P.; Yang, H.; Zhang, M.; Wang, Z. T.; Hao, X. J. *Acta Pharm. Sin.* **2003**, *38*, 924−926.
(10) Cane, D. E. *Chem. Rev.* **1990**, *90*, 1089−1103.
(11) Dewick, P. M. *Nat. Prod. Rep.* **2002**, *19*, 181−222.
(12) Neuhaus, D.; Williamson, M. P. *The Nuclear Overhause Effect in Structural and Conformational Analysys*, 2nd ed.; Wiley-VCH: Weinheim, Germany, 2000.
(13) Böttcher, B.; Thiele, C. M. *eMagRes.* **2012**, *1*, 169−180.
(14) Gil, R. R.; Griesinger, C.; Navarro-Vázquez, A.; Sun, H. *Structure Elucidation in Organic Chemistry*; Wiley-VCH Verlag GmbH & Co.: KGaA, 2015; pp 279−324.
(15) Kummerlöwe, G.; Luy, B. *Annu. Rep. NMR Spectrosc.* **2009**, *68*, 193−232.
(16) García, M. E.; Pagola, S.; Navarro-Vázquez, A.; Phillips, D. D.; Gayathri, C.; Krakauer, H.; Stephens, P. W.; Nicotra, V. E.; Gil, R. R. *Angew. Chem., Int. Ed.* **2009**, *48*, 5670−5674.
(17) Waratchareeyakul, W.; Hellemann, E.; Gil, R. R.; Chantrapromma, K.; Langat, M. K.; Mulholland, D. A. *J. Nat. Prod.* **2017**, *80*, 391−402.
(18) Mevers, E.; Saurí, J.; Liu, Y.; Moser, A.; Ramadhar, T.; Varlan, M.; Williamson, R.; Martin, G.; Clardy, J. *J. Am. Chem. Soc.* **2016**, *138*, 12324−12327.
(19) Gil, R. R.; Gayathri, C.; Tsarevsky, N.; Matyjaszewski, K. *J. Org. Chem.* **2008**, *73*, 840−848.
(20) Castañar, L.; García, M.; Hellemann, E.; Nolis, P.; Gil, R. R.; Parella, T. *J. Org. Chem.* **2016**, *81*, 11126−11131.
(21) Navarro-Vázquez, A.; Gil, R. R.; Blinov, K. *J. Nat. Prod.* **2018**, *81*, 203−210.
(22) Troche-Pesqueira, E.; Anklin, C.; Gil, R. R.; Navarro-Vázquez, A. *Angew. Chem., Int. Ed.* **2017**, *56*, 3660−3664.
(23) *StereoFitter 1.0-beta, MestReLab Research S. L.*; Santiago de Compostela, Spain, 2018.
(24) Frisch, M. J.; Trucks, G. W.; Schlegel, H. B.; Scuseria, G. E.; Robb, M. A.; Cheeseman, J. R.; Scalmani, G.; Barone, V.; Mennucci, B.; Petersson, G. A.; Nakatsuji, H.; Caricato, M.; Li, X.; Hratchian, H. P.; Izmaylov, A. F.; Bloino, J.; Zheng, G.; Sonnenberg, J. L.; Hada, M.; Ehara, M.; Toyota, K.; Fukuda, R.; Hasegawa, J.; Ishida, M.; Nakajima, T.; Honda, Y.; Kitao, O.; Nakai, H.; Vreven, T.; Montgomery, J. A., Jr.; Peralta, J. E.; Ogliaro, F.; Bearpark, M. J.; Heyd, J.; Brothers, E. N.; Kudin, K. N.; Staroverov, V. N.; Kobayashi, R.; Normand, J.; Raghavachari, K.; Rendell, A. P.; Burant, J. C.; Iyengar, S. S.; Tomasi, J.; Cossi, M.; Rega, N.; Millam, N. J.; Klene, M.; Knox, J. E.; Cross, J. B.; Bakken, V.; Adamo, C.; Jaramillo, J.; Gomperts, R.; Stratmann, R. E.; Yazyev, O.; Austin, A. J.; Cammi, R.; Pomelli, C.; Ochterski, J. W.; Martin, R. L.; Morokuma, K.; Zakrzewski, V. G.; Voth, G. A.; Salvador, P.; Dannenberg, J. J.; Dapprich, S.; Daniels, A. D.; Farkas, Ö.; Foresman, J. B.; Ortiz, J. V.; Cioslowski, J.; Fox, D. J. *Gaussian 09*, Revision A.02; Gaussian Inc.: Wallingford, CT, 2016.
(25) Akaike, H. *IEEE Trans. Autom. Control* **1974**, *19*, 716−723.
(26) Berdagué, P.; Herbert-Pucheta, J.; Jha, V.; Panossian, A.; Leroux, F.; Lesot, P. *New J. Chem.* **2015**, *39*, 9504−9517.
(27) Naya, K.; Takagi, I.; Kawaguchi, Y.; Asada, Y.; Hirose, Y.; Shinoda, N. *Tetrahedron* **1968**, *24*, 5871−5879.
(28) Ahmed, A. A. *J. Nat. Prod.* **1991**, *54*, 271−272.
(29) Ruiz-Vásquez, L.; Olmeda, A. S.; Zúñiga, G.; Villarroel, L.; Echeverri, L. F.; González Coloma, A.; Reina, M. *Chem. Biodiversity* **2017**, *14*, 1−9.
(30) Arciniegas, A.; Pérez Castorena, A. L.; Reyes, S.; Contreras, J. L.; Romo de Vivar, A. *J. Nat. Prod.* **2003**, *66*, 225−229.
(31) Xu, J. Q.; Hu, L- H. *Helv. Chim. Acta* **2009**, *92*, 357−361.
(32) Bohlmann, F.; Knoll, K. H. *Liebigs Ann. Chem.* **1979**, *1979*, 470−472.
(33) Naya, K.; Tsuji, K.; Haku, U. *Chem. Lett.* **1972**, *1*, 235−236.
(34) Budesinsky, M.; Holub, M.; Saman, D.; Smitalova, Z.; Ulubelen, A.; Oksuz, S. *Collect. Czech. Chem. Commun.* **1984**, *49*, 1311−1317.
(35) Loyola, L. A.; Pedreros, S.; Morales, G. *Phytochemistry* **1985**, *24*, 1600−1602.
(36) Urones, J. G.; Teresa, J. P.; Marcos, I. S.; Fernández Moro, R.; Basabe Barcala, P.; Cuadrado, J. S. *Phytochemistry* **1987**, *26*, 1113−1115.
(37) Segall, H. J. *J. Liq. Chromatogr.* **1979**, *9*, 1319−1323.
(38) Gu, J. Q.; Wang, Y.; Franzblau, S. G.; Montenegro, G.; Timmermann, B. N. *J. Nat. Prod.* **2004**, *67*, 1483−1487.
(39) Yang, J. L.; Wang, R.; Shi, Y. P. *Nat. Prod. Bioprospect.* **2011**, *1*, 1−24.
(40) Beattie, K. D.; Waterman, P. G.; Forster, P. I.; Thompson, D. R.; Leach, D. N. *Phytochemistry* **2011**, *72*, 400−408.
(41) Shoemaker, R. H. *Nat. Rev. Cancer* **2006**, *6*, 813−823.
(42) Thiele, C. M.; Bermel, W. J. *J. Magn. Reson.* **2012**, *216*, 134−143.
(43) *Ligprep, Schrodinger Release 2017-3*; Schrodinger LLC, New York, 2017.
(44) Halgren, T. A. J. *J. Comput. Chem.* **1996**, *17*, 490−519.
(45) Chang, G.; Guida, W. C.; Still, W. C. *J. Am. Chem. Soc.* **1989**, *111*, 4379−4386.
(46) *MacroModel Schrodinger release 2017-3*; Schrodinger LLC: New York, 2017.
(47) Forsyth, D. A.; Sebag, A. B. *J. Am. Chem. Soc.* **1997**, *119*, 9483−9494.

DOI: 10.1021/acs.jnatprod.8b00162
J. Nat. Prod. XXXX, XXX, XXX−XXX